

Electronic Supplementary Information (ESI) for ChemComm

Simultaneous self-assembly of a cage-like silver(I) complex encapsulating an Ag₆ neutral cluster core and carbon dioxide fixation

Di Sun,^a Geng-Geng Luo,^c Na Zhang,^a Rong-Bin Huang,^{*a} Lan-Sun Zheng^b

^aDepartment of chemistry, College of Chemistry and Chemical Engineering, Xiamen University, Xiamen 361005, China. E-mail: rbhuang@xmu.edu.cn

^bState key Laboratory for Physical Chemistry of Solid Surfaces, Xiamen University, Xiamen 361005, China

^cInstitute of Materials Physical Chemistry, Huaqiao University, Quanzhou, Fujian 362021, China

Content

(1) Materials and methods.....	2
(2) Synthesis of 1-3	3
(3) X-ray crystallography	4
(4) Description of crystal structures of 2 and 3.....	6
Structure of 2	6
Structure of 3	7
(5) Figure S1. Ortep drawing molecule structure of 2	8
(6) Figure S2. Ortep drawing of two different dimers in 3	9
(7) Figure S3 An ORTEP drawing of crystal packing diagram of 3 viewed along <i>a</i> axis.....	10
(8) Figure S4 Energy dispersive X-ray spectroscopy (EDS) data for 1 showing the existence of Cl element.....	11
(9) Figure S5 The photograph of crystal of 1.....	12
(10) Figure S7. Narrow-scan Ag 3d _{5/2} XPS spectrum.....	13
(11) Figure S8. The color change of filtrate in air in three hours.....	14
(12) Figure S9 UV-Vis spectral changes for filtrate in air.....	15
(13) Figure S10. PXRD spectroscopy for black precipitate and typical SEM image	16
(14) Table S1. Crystallographic Data for 1-3	17
(15) Table S2. Bond Distances (Å) and Angles (°) for 1.....	18
(16) Table S3. Bond Distances (Å) and Angles (°) for 2.....	19
(17) Table S4. Bond Distances (Å) and Angles (°) for 3.....	20
(18) Figure S11. TGA curve of 1.....	21

(1) Materials and methods

All of the reagents and solvents employed were commercially available and used as received without further purification. The FT-IR spectra were recorded from KBr pellets in the range 4000-400 cm⁻¹ with a Nicolet AVATAR FT-IR360 spectrometer. EPR spectra were taken on a Bruker EMX 10/12 Electron Spin Resonance Spectrometer. UV/Vis absorption spectra were determined on a Beckman DU-7400 spectrophotometer. Energy dispersive X-ray spectra were obtained on HITACHI S-4800 scanning electron microscope, which is equipped with an HORIBA EDS unit. X-ray photoelectron spectra (XPS) were recorded with a Quantum 2000 X-ray scanning ESCA microprobe. The single crystals were put under UHV to reach the 10⁻⁸ Pa range. The nonmonochromatized Al *K*_a source was used at 10 kV and 10 mA. The binding energy of the spectrum was calibrated in relation to the C 1s binging energy (284.0 eV), which was applied as an internal standard. High resolution narrow-scan spectra were recorded with the electron pass energy of 50 eV and takeoff angle of 55° to achieve the maximum spectral resolution. The narrow scans spectra were deconvoluted using the peakfit software (XPSPEAK 4.1) to reveal the different oxidation states of Ag in **1**. Nonlinear least squares curve fitting was performed using a Gaussian/Lorentzian peak shape after background removal. Powder X-ray diffraction (PXRD) data were collected on a Philips X’Pert Pro MPD X-ray diffractometer with Cu *K*_a ($\lambda = 1.5418 \text{ \AA}$, 40.0 kV, 30.0 mA) radiation equipped with an X’Celerator detector. The C, H and N microanalyses were carried out with a CE instruments EA 1110 elemental analyzer. TG curves were measured from 25 to 700 °C on a SDT Q600 instrument at a heating rate 5 °C/min under the N₂ atmosphere (100 ml/min).

CAUTION! Perchlorate salts in the presence of organic ligands are potentially explosive and heating has to be avoided. Only small amounts of the materials should be prepared, and handled with care.

(2) Synthesis of 1-3

[Ag₃₄(dppm)₁₂(CO₃)₁₂Cl₄] (1·164DMF): Reaction of Ag₂O (116 mg, 0.5 mmol), NH₂dmpym (124 mg, 1 mmol), dppm (192mg, 0.5 mmol) and NaClO₄·H₂O (140 mg, 1 mmol) in DMF/CH₃CN (16 mL, v/v 3:5) in the presence of ammonia (25%, 0.5 mL) in air under ultrasonic treatment (160 W, 40 KHz, 50 °C, 20 min). At first a pale yellow filtrate was obtained by filtration, after one day standing, the color obviously changed to dark brown. The finally clear solution was obtained by filtration again and allowed to slowly evaporate in darkness in constant environment (38°C) for one week to give colorless block crystals of **1**. The crystals were collected by filtration and dried at room temperature. Yield: *Ca.* 34% (98 mg) based on Ag. Selected IR peaks (cm⁻¹): 3400(s), 3053(m, Ar-H), 1666(m), 1465 (m), 1437(s), 877(w), 736(s), 716(s), 693(s), 668(w), 526(s), 510(s), 479(m).

For DMF/CH₃CN (16mL, v/v 3:5) solvents system, the pH of pale yellow filtrate by firstly filtrating is very high, *ca.* 13.6, after one day standing, the pH of finally clear solution obtained by filtration again decrease to *ca.* 11.4.

[Ag₂(dppa)(dppm)(ClO₄)₂·2DMF (2): **2** is a byproduct in the process of synthesis of **1**. After obtaining compound **1** by filtration, the rest mother liquor was left in the constant environment (38 °C) again, after about two weeks, the yellow plate crystals of **2** was obtained. The crystals were collected by filtration and dried at room temperature. Yield: *Ca.* 16% (48 mg) based on Ag. Selected IR peaks (cm⁻¹): 3400(s), 3050(m, Ar-H), 1471(m), 1081(s, ClO₄⁻), 950(s), 940(s), .738(s), 725(s), 520(w), 508(w), 485(w).

[Ag₂(dppm)(NHdmpym)(ClO₄)₂ (3): Synthesis of **3** is the similar to that of **1**, but synthesis and crystallization of **3** were conducted under N₂ atmosphere, the yellow plate crystals of **3** were obtained in three days. Yield: *Ca.* 58% (238 mg) based on Ag. Selected IR peaks (cm⁻¹): 3331(s), 3049(w, Ar-H), 1590(m), 1436(s), 1382(m), 1106(s, ClO₄⁻).745(s), 725(s).

(3) X-ray crystallography

Data was collected on a Siemens SMART CCD diffractometer with monochromatic Mo $K\alpha$ radiation ($\lambda = 0.71073 \text{ \AA}$) for **1-3** [hemisphere data collection in ω at 0.3° scan width in three runs with 600, 435, and 230 frames ($\phi = 0, 88,$ and 180°) at a detector distance of 6 cm]. Complex **1** crystallizes in the rare cubic space group $Fd\bar{3}$ (No. 203). The unit cell parameters of **1** are the maximum in all complexes with $Fd\bar{3}$ space group which are comparable to those found in macromolecules ($a \approx 54 \text{ \AA}$). All absorption corrections were performed with the SADABS program [S1]. All the structures were solved by direct methods using SHELXS-97 [S2] and refined by full-matrix least-squares techniques using SHELXL-97 [S3]. All the non-hydrogen atoms were treated anisotropically, with the exception of atoms O7, N1, C38-C40 belonging to a disordered DMF molecule in complex **2**, which were refined with isotropic thermal parameters. The positions of hydrogen atoms were generated geometrically. The crystallographic details of **1-3** are summarized in Table S1.

There are large solvent accessible void volumes in the crystals of **1** which are occupied by highly disordered DMF molecules. No satisfactory disorder model could be achieved, and therefore the SQUEEZE program [S4] implemented in PLATON was used to remove these electron densities. The SQUEEZE function of the program PLATON reveals a residual electron density of 52698 electrons/cell in cell-remaining voids where the residual electron density was tentatively assigned to 164 molecules of the DMF solvent [$52682/8 = 6585$ for per formula of **1**; $6560 = 40 \text{ (DMF)} \times 164$]. The number of DMF was also proved by the TGA and EA (Fig. S11). The TENTATIVE formula for **1** is $[\text{Ag}_{34}(\text{dppm})_{12}(\text{CO}_3)_{12}\text{Cl}_4] \cdot 164\text{DMF}$. A refinement using reflections modified by the SQUEEZE procedure behaved well, and the R_1 were significantly reduced from 0.12 to 0.07.

References

- [S1] G. M. Sheldrick, *SADABS. Program for Absorption Correction of Area Detector Frames*, Bruker AXS Inc., Madison, Wisconsin, USA.
- [S2] G. M. Sheldrick, *SHELXS 97: Program for Crystal Structure Solution*, University of Göttingen: Göttingen, Germany, 1997.
- [S3] G. M. Sheldrick, *SHELXL 97: Program for Crystal Structure refinement*, University of

Supplementary Material (ESI) for Chemical Communications
This journal is (c) The Royal Society of Chemistry 2010

Göttingen: Göttingen, Germany, 1997.

[S4] A. L. Spek, *J. Appl. Crystallogr.*, 2003, **36**, 7.

(4) Description of crystal structures of **2** and **3**

Structure of **2**

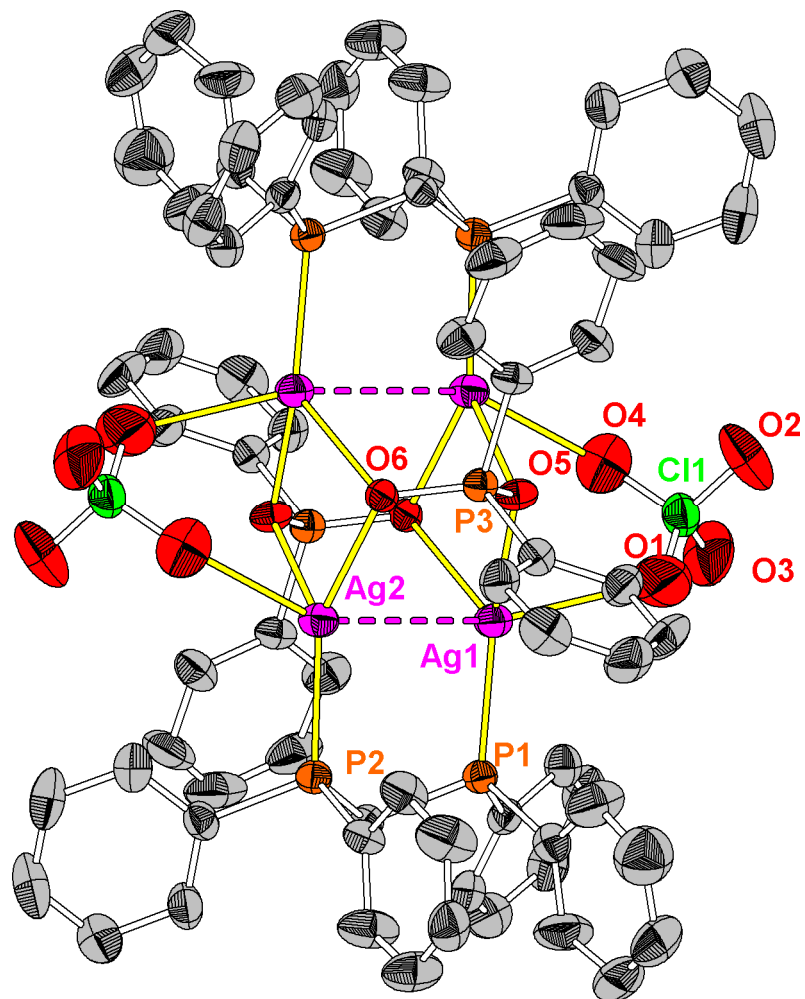
It should be noted that the cleavage of P–C bond indicates that the dppm ligand is oxidized in our reaction system and is a potential reductant of ClO_4^- . The infrared spectrum of **2** displays typical absorption peaks at 950 and 940 cm^{-1} , which are characteristic for $\nu_{(\text{P}-\text{O})}$ stretching vibration of the coordinated $[\text{Ph}_2\text{PO}_2]^-$.

As shown in Fig. S1, each Ag^{l} ion is tetrahedrally coordinated by three oxygen atoms and one phosphorus atom. Three kinds of bridging ligands surround the Ag_4 square unit: two $[\text{Ph}_2\text{PO}_2]^-$ ligands exhibiting a μ_4 -coordinantion mode are bonded from both sides of the Ag_4 plane and are perpendicular to each other, while two dppm ligands and two $\mu_2\text{-}\text{ClO}_4^-$ anions bridge the edges of Ag_4 in opposite directions. The distances of the $\text{Ag}\cdots\text{Ag}$ separation bridged by μ_2 -dppm ligands and $\mu_2\text{-}\text{ClO}_4^-$ anions in **2** are 3.2192(14) and 3.555(1) Å, respectively. In the whole, the $\pi\cdots\pi$ stacking interactions and C–H $\cdots\pi$ interactions are contributed to the stability of the crystal packing.

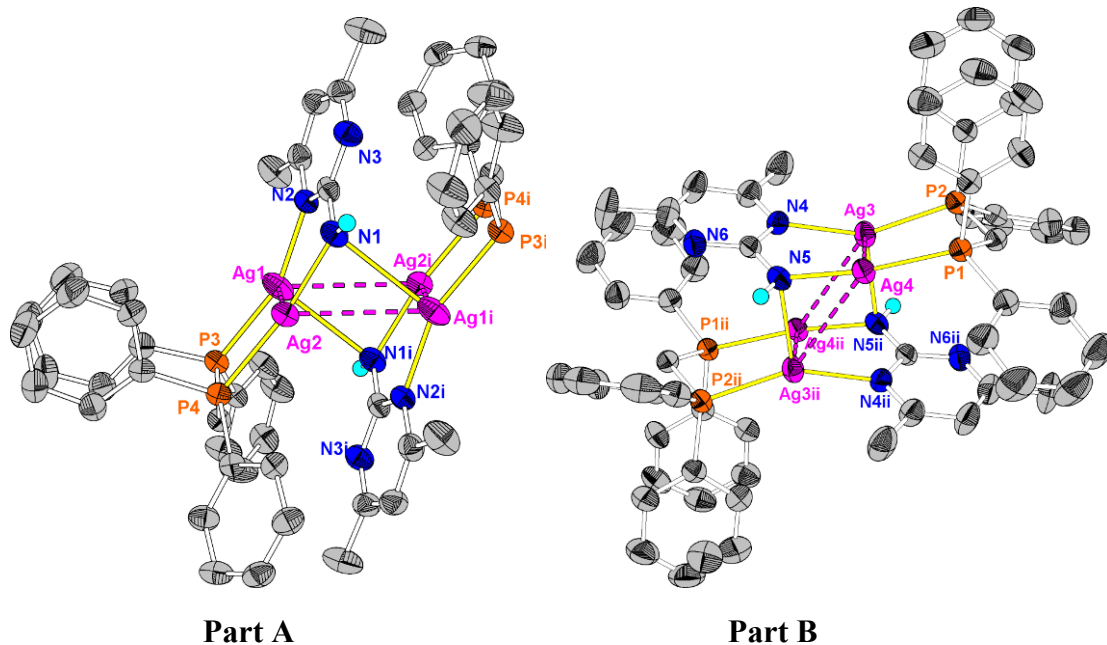
Structure of 3

Single-crystal X-ray diffraction analysis shows the occurrence of two kinds of dimers within an asymmetric unit (Figure S2, herein designated as part A and B). Selected bond lengths and angles are given in Table S4. In each dimer, four Ag^I ions form an Ag₄ square geometry, and the crystallographic inversion center locates on the centre of Ag₄ square. The shortest Ag···Ag distance is 2.8397 (9) Å which is shorter than the Ag···Ag distance in metallic Ag (2.886 Å). Interestingly, deprotonated amino groups of NH₂dmpym ligand adopt μ_1 and μ_2 coordination modes to bridge Ag^I atoms to form dimer A and B, respectively, which is the first example in the silver/NH₂dmpym system showing the unprecedented bridging mode of NH₂dmpym. In the whole, the C-H···O (ClO₄⁻) hydrogen bonds contributed to the stability of the crystal packing.

(5) Figure S1. Ortep drawing molecule structure of 2



(6) Figure S2. Ortep drawing of two different dimers in 3

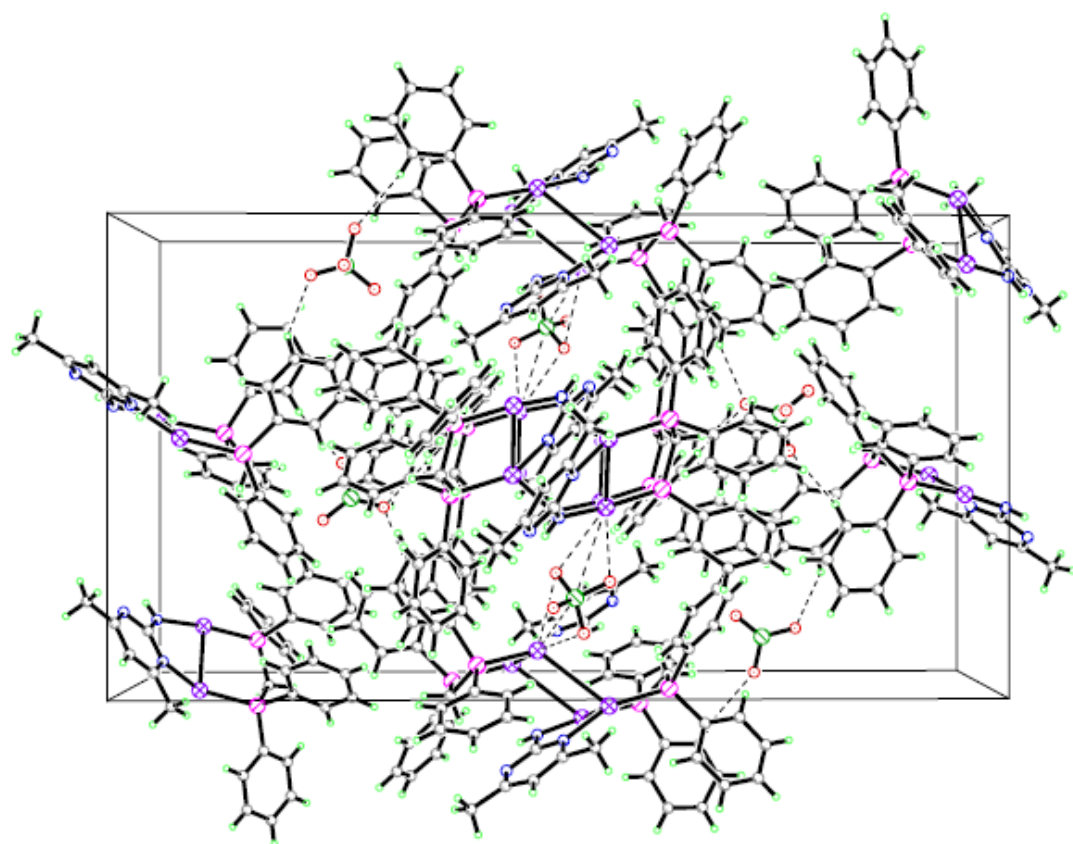


Part A

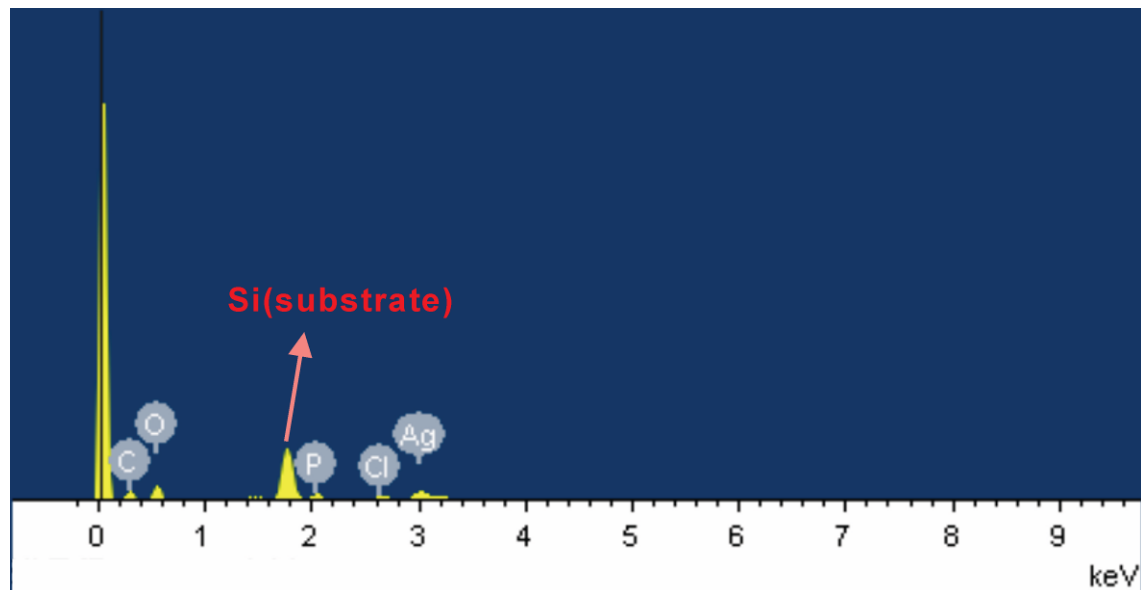
Part B

Hydrogen atoms on carbon atoms and ClO_4^- are omitted for clarity. (Symmetry codes: (i):
 $1-x, 1-y, -z$; (ii): $-x, -y, -z$).

(7) Figure S3 An ORTEP drawing of crystal packing diagram of 3 viewed along *a* axis.



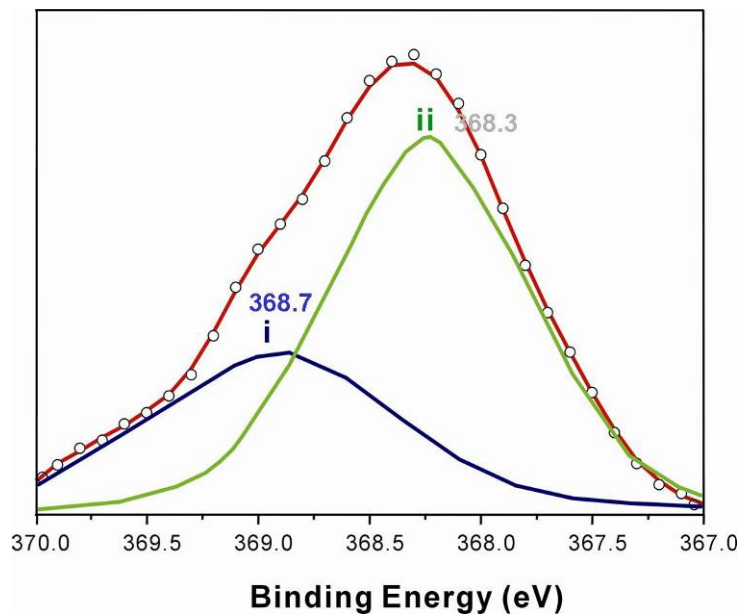
(8) Figure S4 Energy dispersive X-ray spectroscopy (EDS) data for 1 showing the existence of Cl element.



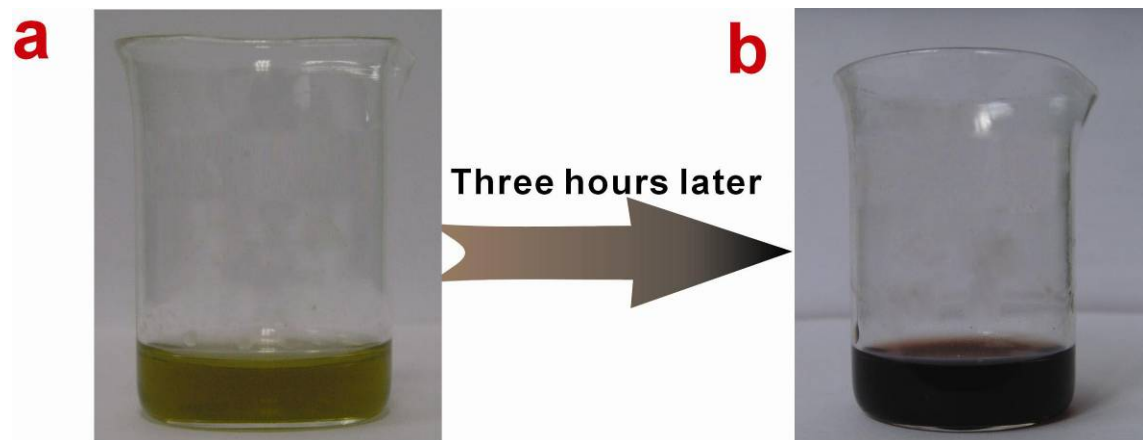
(9) Figure S5 The photograph of crystal of 1.



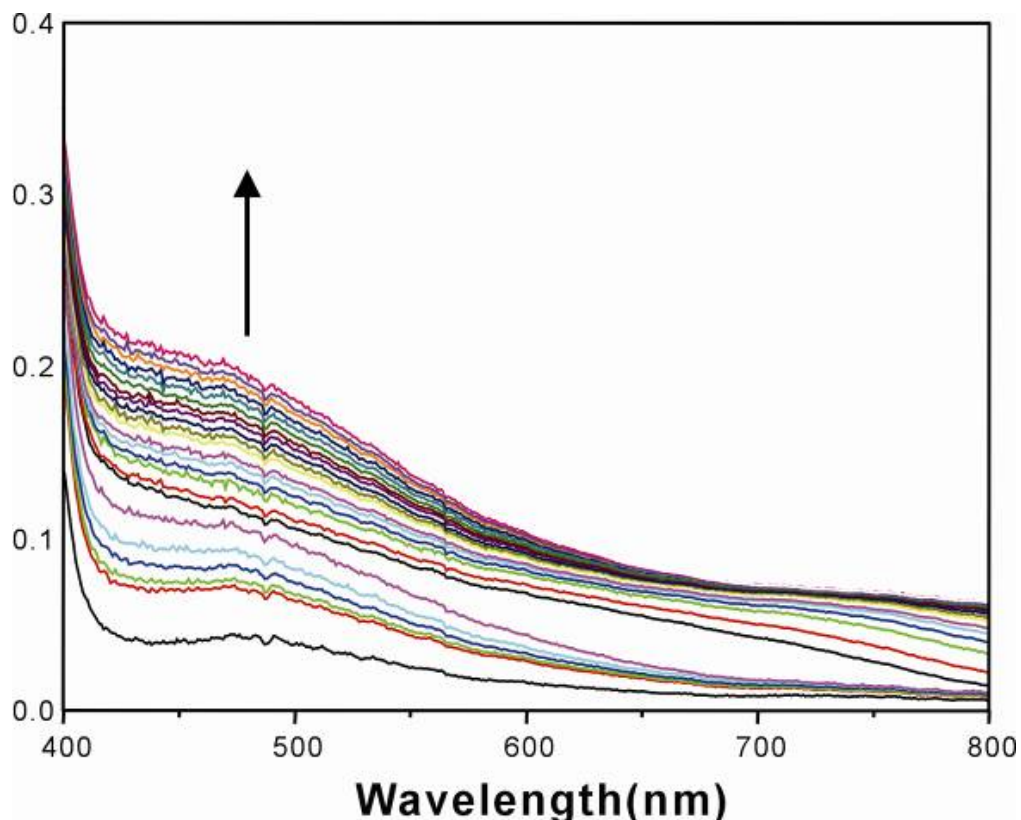
(10) Figure S7. Narrow-scan Ag 3d_{5/2} XPS spectrum



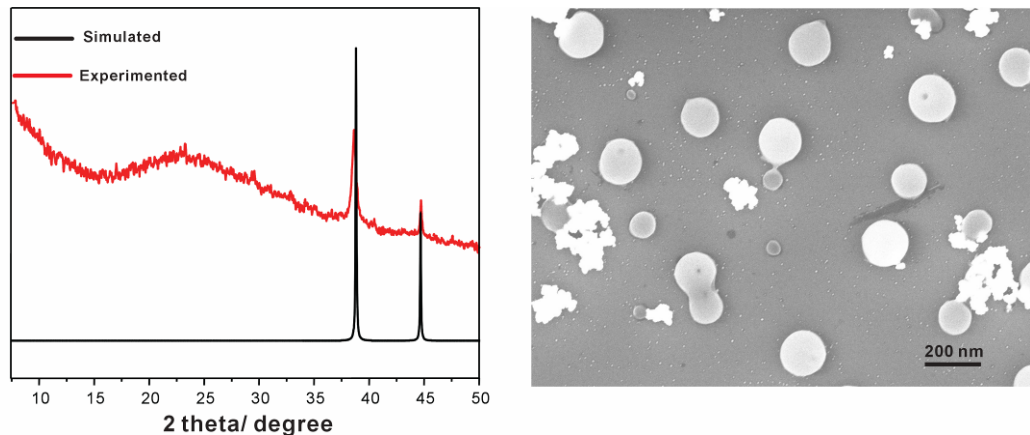
(11) Figure S8. The color change of filtrate in air in three hours



(12) Figure S9 UV-Vis spectral changes for filtrate in air.



(13) Figure S10. PXRD spectroscopy for black precipitate and typical SEM image



(14) Table S1. Crystallographic Data for 1-3

Complexes	1	2	3
Formula	C ₃₁₂ H ₂₆₄ Ag ₃₄ Cl ₄ O ₃₆ P ₂₄	C ₈₀ H ₇₈ Ag ₄ Cl ₂ N ₂ O ₁₄ P ₆	C ₆₂ H ₆₀ Ag ₄ Cl ₂ N ₆ O ₈ P ₄
M _r	9141.89	1979.64	1643.44
Crystal system	Cubic	Monoclinic	Monoclinic
Space group	<i>Fd</i> 3̄	<i>P2</i> ₁ /n	<i>P2</i> ₁ /c
a (Å)	54.274(6)	11.453(2)	12.670(3)
b (Å)	54.274(6)	15.193(3)	16.694(3)
c (Å)	54.274(6)	23.416(5)	30.990(6)
α (deg)	90	90	90
β (deg)	90	97.14(3)	91.75(3)
γ (deg)	90	90	90
Z	8	2	2
V (Å ³)	159876(32)	4043.2(14)	6552(2)
D _c (g cm ⁻³)	0.760	1.626	1.666
μ(mm ⁻¹)	0.897	1.203	1.414
F(000)	35600	1992	3280
no. of unique reflns	11717	7115	12870
no. of obsd	2790	4170	8957
reflns[I > 2σ(I)]			
Parameters	309	492	775
Final R indices [I > 2σ(I) ^{a,b}	R ₁ = 0.0742, wR ₂ = 0.2008	R ₁ = 0.0837, wR ₂ = 0.2307	R ₁ = 0.0423, wR ₂ = 0.1178
R indices (all data)	R ₁ = 0.1782, wR ₂ = 0.2328	R ₁ = 0.1325 wR ₂ = 0.2748	R ₁ = 0.0617 wR ₂ = 0.1348
Δρ (e Å ⁻³)	0.441 and -0.315	3.852 and -1.323	1.271 and -0.812

^aR₁ = $\sum ||F_o| - |F_c|| / \sum |F_o|$. ^bwR₂ = $[\sum w(F_o^2 - F_c^2)^2 / \sum w(F_o^2)^2]^{0.5}$.

(15) Table S2. Bond Distances (Å) and Angles (°) for 1

Ag1—O3 ⁱ	2.288 (8)	Ag2—Ag3	2.9243 (16)
Ag2—Ag2 ^{vii}	3.113 (2)	Ag3—O2	2.348 (8)
Ag1—Ag1 ⁱⁱⁱ	2.795 (2)	Ag3—P1	2.386 (4)
Ag3—O2 ⁱⁱ	2.483 (8)	Ag3—Cl1	2.629 (3)
Ag1—Ag1 ^{vi}	2.795 (2)	Ag4—O1	2.282 (8)
Ag2—O3 ⁱⁱ	2.196 (8)	Ag4—Ag1 ^{vi}	3.0027 (16)
Ag2—P2	2.307 (4)	Ag2—O1	2.334 (8)
O3 ⁱ —Ag1—O3 ⁱⁱ	73.9 (4)	P2—Ag2—Ag3	92.14 (10)
O3 ⁱ —Ag1—Ag1 ⁱⁱⁱ	167.8 (2)	O1—Ag2—Ag3	77.7 (2)
O3 ⁱⁱ —Ag1—Ag1 ⁱⁱⁱ	98.8 (2)	O3 ⁱⁱ —Ag2—Ag2 ^{vii}	58.78 (19)
O3 ⁱ —Ag1—Ag1 ^{iv}	132.00 (19)	P2—Ag2—Ag2 ^{vii}	106.62 (10)
O3 ⁱⁱ —Ag1—Ag1 ^{iv}	117.46 (18)	O1—Ag2—Ag2 ^{vii}	123.6 (2)
Ag1 ⁱⁱⁱ —Ag1—Ag1 ^{iv}	60.0	Ag3—Ag2—Ag2 ^{vii}	135.35 (6)
O3 ⁱ —Ag1—Ag1 ^v	117.46 (18)	O2—Ag3—P1	133.0 (2)
O3 ⁱⁱ —Ag1—Ag1 ^v	132.00 (19)	O2—Ag3—O2 ⁱⁱ	88.4 (4)
Ag1 ⁱⁱⁱ —Ag1—Ag1 ^v	60.0	P1—Ag3—O2 ⁱⁱ	133.7 (2)
Ag1 ^{iv} —Ag1—Ag1 ^v	90.0	O2—Ag3—Cl1	86.0 (2)
O3 ⁱ —Ag1—Ag1 ^{vi}	98.8 (2)	P1—Ag3—Cl1	114.21 (14)
O3 ⁱⁱ —Ag1—Ag1 ^{vi}	167.8 (2)	O2 ⁱⁱ —Ag3—Cl1	83.3 (2)
Ag1 ⁱⁱⁱ —Ag1—Ag1 ^{vi}	90.0	O2—Ag3—Ag2	84.3 (2)
Ag1 ^{iv} —Ag1—Ag1 ^{vi}	60.0	P1—Ag3—Ag2	89.23 (10)
Ag1 ^v —Ag1—Ag1 ^{vi}	60.0	O2 ⁱⁱ —Ag3—Ag2	73.15 (19)
O3 ⁱ —Ag1—Ag4 ^{vii}	105.6 (2)	Cl1—Ag3—Ag2	154.71 (11)
O3 ⁱⁱ —Ag1—Ag4 ^{vii}	69.74 (19)	O1 ⁱ —Ag4—O1	119.971 (11)
Ag1 ⁱⁱⁱ —Ag1—Ag4 ^{vii}	62.27 (3)	Ag1 ^{iv} —Ag1—Ag4 ^{vii}	122.24 (3)
Ag1 ^v —Ag1—Ag4 ^{vii}	62.27 (3)	O1 ⁱ —Ag4—Ag1	78.72 (19)
Ag1 ^{vi} —Ag1—Ag4 ^{vii}	122.24 (3)	O1—Ag4—Ag1	72.0 (2)
O3 ⁱ —Ag1—Ag4	69.74 (19)	O1 ^{viii} —Ag4—Ag1	123.2 (2)
O3 ⁱⁱ —Ag1—Ag4	105.6 (2)	O1 ⁱ —Ag4—Ag1 ^{iv}	123.2 (2)
Ag1 ^{iv} —Ag1—Ag4	62.27 (3)	O1 ^{viii} —Ag4—Ag1 ^{iv}	72.0 (2)
Ag4 ^{vii} —Ag1—Ag4	174.48 (6)	O1—Ag4—Ag1 ^{vi}	123.2 (2)
O3 ⁱⁱ —Ag2—P2	157.1 (2)	O1 ^{viii} —Ag4—Ag1 ^{vi}	78.72 (19)
O3 ⁱⁱ —Ag2—O1	85.0 (3)	Ag1—Ag4—Ag1 ^{vi}	55.47 (5)
P2—Ag2—O1	117.6 (2)	Ag1 ^{iv} —Ag4—Ag1 ^{vi}	55.47 (5)
O3 ⁱⁱ —Ag2—Ag3	88.85 (18)		

Symmetry codes: (i) $y, -z+5/4, -x+5/4$; (ii) $-y+5/4, -z+5/4, x$; (iii) $-y+5/4, z, -x+5/4$; (iv) $z, -x+5/4, -y+5/4$; (v) z, x, y ; (vi) y, z, x ; (vii) $-x+5/4, y, -z+5/4$; (viii) $-z+5/4, x, -y+5/4$.

(16) Table S3. Bond Distances (Å) and Angles (°) for 2

Ag1—O5	2.246 (7)	Ag2—O6	2.284 (6)
Ag1—P1	2.369 (3)	Ag2—P2	2.375 (3)
Ag1—O6 ⁱ	2.508 (7)	Ag2—O5 ⁱ	2.412 (7)
Ag1—Ag2	3.2192 (14)		
O5—Ag1—P1	154.16 (19)	O6—Ag2—P2	150.62 (19)
O5—Ag1—O6 ⁱ	79.5 (2)	O6—Ag2—O5 ⁱ	80.8 (2)
P1—Ag1—O6 ⁱ	122.99 (16)	P2—Ag2—O5 ⁱ	125.34 (17)
O5—Ag1—Ag2	81.08 (19)	O6—Ag2—Ag1	82.31 (18)
P1—Ag1—Ag2	88.72 (7)	P2—Ag2—Ag1	88.36 (7)
O6 ⁱ —Ag1—Ag2	83.15 (16)	O5 ⁱ —Ag2—Ag1	81.54 (18)
Symmetry codes: (i) $-x+2, -y+2, -z$.			

(17) Table S4. Bond Distances (\AA) and Angles ($^\circ$) for 3

Ag1—N2	2.157 (4)	Ag3—N4	2.197 (5)
Ag1—P3	2.3710 (15)	Ag3—P2	2.3897 (15)
Ag1—Ag2	2.8397 (9)	Ag3—N5 ⁱⁱ	2.539 (5)
Ag1—Ag2 ⁱ	3.3311 (9)	Ag3—Ag4	2.8871 (7)
Ag2—N1	2.104 (4)	Ag4—N5	2.106 (5)
Ag2—P4	2.3619 (15)	Ag4—P1	2.3604 (16)
N2—Ag1—P3	160.02 (13)	Ag1—Ag2—Ag1 ⁱ	89.67 (3)
N2—Ag1—Ag2	85.11 (12)	N4—Ag3—P2	150.76 (13)
P3—Ag1—Ag2	96.60 (4)	N4—Ag3—N5 ⁱⁱ	107.07 (16)
N2—Ag1—Ag2 ⁱ	72.06 (12)	P2—Ag3—N5 ⁱⁱ	102.16 (11)
P3—Ag1—Ag2 ⁱ	127.71 (5)	N4—Ag3—Ag4	83.80 (13)
Ag2—Ag1—Ag2 ⁱ	90.33 (3)	P2—Ag3—Ag4	92.53 (4)
N1—Ag2—P4	166.33 (13)	N5 ⁱⁱ —Ag3—Ag4	99.02 (11)
N1—Ag2—Ag1	79.13 (13)	N5—Ag4—P1	169.24 (14)
P4—Ag2—Ag1	88.72 (4)	N5—Ag4—Ag3	78.23 (14)
N1—Ag2—Ag1 ⁱ	57.29 (14)	P1—Ag4—Ag3	92.19 (4)
P4—Ag2—Ag1 ⁱ	129.59 (4)		

Symmetry codes: (i) $-x+1, -y+2, -z+1$; (ii) $-x, -y+1, -z+1$.

(18) Figure S11. TGA curve of 1.

